

Lawrence Berkeley National Laboratory

Recent Work

Title

DESIGN CONSIDERATIONS FOR A LIMPED SOLENOID

Permalink

<https://escholarship.org/uc/item/9cx5t8mp>

Author

Halbach, Klaus.

Publication Date

1975-08-01

Presented at the 1975 PEP Summer Study,
Lawrence Berkeley Lab., Berkeley, CA,
July 28 - August 20, 1975

RECEIVED
LIBRARY AND
DOCUMENTS SECTION

LBL-4270

c. |

DEC 4 1975

LIBRARY AND
DOCUMENTS SECTION

DESIGN CONSIDERATIONS FOR A LUMPED SOLENOID

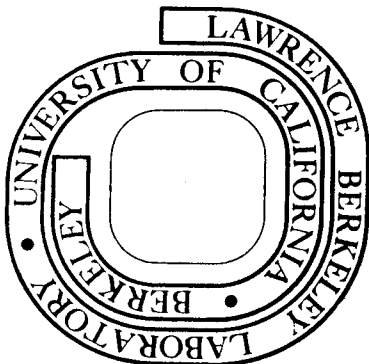
Klaus Halbach

August 1975

Prepared for the U. S. Energy Research and
Development Administration under Contract W-7405-ENG-48

For Reference

Not to be taken from this room



LBL-4270

c. |

U C B L 4 2 7 0

DISCLAIMER

This document was prepared as an account of work sponsored by the United States Government. While this document is believed to contain correct information, neither the United States Government nor any agency thereof, nor the Regents of the University of California, nor any of their employees, makes any warranty, express or implied, or assumes any legal responsibility for the accuracy, completeness, or usefulness of any information, apparatus, product, or process disclosed, or represents that its use would not infringe privately owned rights. Reference herein to any specific commercial product, process, or service by its trade name, trademark, manufacturer, or otherwise, does not necessarily constitute or imply its endorsement, recommendation, or favoring by the United States Government or any agency thereof, or the Regents of the University of California. The views and opinions of authors expressed herein do not necessarily state or reflect those of the United States Government or any agency thereof or the Regents of the University of California.

DESIGN CONSIDERATIONS FOR A LUMPED SOLENOID*

Klaus Halbach
Lawrence Berkeley Laboratory
University of California
Berkeley, California 94702

1. Introduction

This note is primarily intended to demonstrate which characteristics of a lumped solenoid (with a steel return path that may also be lumped) are important for good performance. This understanding is clearly necessary to make judgments about trade-offs between qualities of the magnetic field and other desirable attributes of a particular magnet geometry. We also want to show the use of a methodology and some "thinking tools" that can help to obtain the good qualitative understanding of magnetic fields that is necessary for good magnet design, is indispensable for hand calculations, and should be the basis for magnetic field computer runs. While it is clear that it is not possible to say anything basically new along these lines, it seems worthwhile to formulate and state these concepts clearly, since they are not nearly as well known as they ought to be.

To accomplish the stated objective, we first describe the design problem and the general method used to solve it. We then introduce two analog models that often help to get a good qualitative understanding of magnetic fields. In addition, we derive and use a simple formula that can be useful for making quantitative estimates of some properties of magnetic fields. Finally, we apply these methods to the design of the lumped solenoid.

2. The Design Problem and the Methodology Used to Solve It

Fig. B-1 shows a cross-section of the magnet under discussion, with the center line (C_L) representing an axis of cylindrical symmetry. The vertical line at the left represents a symmetry plane. The cross-hatched area indicates the steel that is used to conduct the magnetic flux around the lumped solenoid of radius r_1 , the part at the top of the drawing representing either a cylindrical shell or a cross-section through a "vane" in case one chooses to "lump" that part of the steel structure.

The design goal is the production of a reasonably uniform field over a volume that is not too strongly restricted in either the axial or radial direction. Furthermore the magnetic field should be small in a region outside the coils that begins not too far from the coils.

To understand and assess these problems we start with a discussion of the properties of an idealized magnet (infinite permeability μ , $r_2 = \infty$,

steel everywhere to the right of the dashed line in Fig. B1) and then investigate one by one the effects of the modifications that have to be applied to the idealized magnet in order to obtain the real magnet.

3. Useful Tools and Concepts for the Discussion of Magnetic Fields

It is often quite easy to obtain a good picture of a magnetic field distribution by applying directly the magnetostatic equations, usually in integrated form ($\oint \vec{H} \cdot d\vec{s} = I$, $\oint \vec{B} \cdot d\vec{a} = 0$). However under some circumstances this procedure does not lead easily to a good qualitative feeling for the fields, particularly when one wants to know the fields close to a coil with steel in the vicinity. If the fields have cylindrical symmetry with no component in the azimuthal direction, or if the fields are of a two dimensional nature, the analog model of current flow in a two dimensional conductive sheet often gives the needed insight much more easily. Although this analog model has been used to physically model 2D magnets, B-1 this use is somewhat complicated in the cylindrical case, and the model is used here only as a conceptual aid. Similar comments apply to a slightly different analog model that we use to visualize magnet fields produced by magnetic charges. In both cases the same labels z , r are used for the Cartesian coordinates on the 2D conductive sheet and for the coordinates of the cylindrically symmetric magnets.

An expansion of 2D dipole fields into exponentials will be done in Sect. 3.3. Even though this may seem to be a rather specialized formula, its derivation is reproduced here not only because it is useful for the magnet under discussion, but is, in the authors opinion, the single most important and useful formula (after the magnetostatic equations) for the understanding and design of magnets.

3.1. The Orthogonal Analog Model (OAM)

Inspection of the magnetostatic equations in cylindrical geometry, and of the equations governing the current flow in a two dimensional conductive medium, shows the following relations: (see rows 1 and 2 of Table 1, and also Fig. B-2.

1) If one makes the resistivity $\rho(r,z)$ of the sheet proportional to $r \cdot \mu(r,z)$ (column 1), and

2) If one injects a current density $j_3(r,z)$ into the top surface of the conductive sheet that is proportional to the exciting current density, $j_\phi(r,z)$, in the magnet (column 2),

Then:

3) Scalar equi-potential lines in the model correspond to surfaces of constant rA (i.e., field

*This report has also been included in toto in the PEP Summer Study 1975 Proceedings as Appendix B Figures, references, and tables here retain their B prefixes from the PEP proceedings.

surfaces) in the magnet (column 3), and the vectors \vec{H} and \vec{B} are obtained by rotating the 2D current density vector \vec{j} and electric field vector \vec{E} in the model by 90° (columns 6 and 7).

The table of equivalents for two dimensional magnetic fields is obtained by removing all factors r from Table B-1.

While this treatment of the permeability μ can be advantageous, it is often more convenient to treat finite permeability effects differently:

First μ is assumed to be infinite in order to obtain an understanding of the fields in the vacuum region. From this one learns how magnetic flux enters the steel, leading in turn to a qualitative understanding of the field lines in the steel, and at the steel-vacuum interface. Whenever a field line in the steel at that interface forms a non-zero angle α with the normal to the interface, a non-zero tangential field component $|\vec{H}_t| = \sin \alpha |\vec{B}|/\mu$ exists at that interface. Since that field component is continuous through the interface, it is this component that modifies the field in the vacuum region. Usually, the field produced by this tangential field component H_t is most easily understood if one replaces H_t by a current sheet of strength $I' = |\vec{H}_t|$ on the steel surface. It is easy to see that the current in this sheet points out of (into) the paper plane if the steel lies to the left (right) of the vector \vec{H}_t . The fields produced by these current sheets are in turn often most easily obtained by applying again the OAM.

3.2. The Direct Analog Model (DAM)

In discussing magnetic fields produced by magnetic charges (See Sect. 4.3), it is clear that scalar potentials can be used to describe the properties of the fields. In cylindrical geometry, the radial dependencies become clearer if one uses again a two-dimensional conductive sheet model with the appropriate conductivity and current injection. The equivalences between the quantities in the DAM and a cylindrical magnet are given in rows 2 and 3 of Table B-1, with σ representing the conductivity of the sheet, and q the magnetic charge density in the magnet.

3.3. Expansion of 2D-Dipole Fields into Exponentials

Fig. B-3 shows the cross-section of a magnet assumed to be sufficiently long in the direction perpendicular to the paper plane so that the fields can be considered two-dimensional. We assume further that the magnet has mid-plane symmetry and that $\mu = \infty$ in the steel. As a consequence, the fields are perpendicular to the steel surfaces and the midplane.

To find an expression for the fields that is suitable for our purposes and is valid in the region bounded on top and bottom by the flat part of the pole, we first look at, and graphically represent, how H_y depends on y for $x = 0$ (see Fig. 4): Since $\text{div } \vec{H} = \partial H_x/\partial x + \partial H_y/\partial y = 0$, and $H_x \equiv 0$ for $y = 0$ and $y = \pm g/2$, it follows that $\partial H_y/\partial y = 0$ for $y = 0, y = \pm g/2$. Mid-plane symmetry requires that H_y is an even function of y , and H_x is an odd function of y , leading qualitatively to functions

H_x, H_y as shown in Fig. 4. It follows directly that both H_x and H_y are expandable into Fourier series with period g that should converge quite rapidly since both the functions and at least their first two derivatives with respect to y are continuous. Using the complex representation for these Fourier series, we then form the combination $H^* = H_x - iH_y$ and obtain, by combining the coefficients into an:

$$H^* = H_x - iH_y = \sum_{-\infty}^{\infty} a_n e^{2\pi n i y/g} \quad (1)$$

We have chosen the combination $H_x - iH_y$ because the magnetostatic equations for the vacuum field components H_x and $-H_y$ are the same equations as the Cauchy-Riemann conditions for the real and imaginary part of an analytical function of the complex variable $z = x + iy$. Since we have an explicit expression for the function H^* for the case $x = 0$, we obtain an expression for H^* for $x \neq 0$ by replacing in Eqn. (1) iy by $z = x + iy$. Because $H_x = 0$ in the mid-plane, the coefficients a_n must be purely imaginary. Since the deviations from a uniform field will get smaller as one moves from the left side ($x=0$) or the right side ($x = x_2$) of the magnet toward its center, the terms with $n < 0$ can contribute significantly only on the left side of the magnet, and those with $n > 0$ only on the right side. It is therefore convenient to rewrite Eqn. (1) in the following way:

$$H^* = i(h_0 + \sum_{n=1}^{\infty} h_{-n} e^{-2\pi n z/g} + \sum_{n=1}^{\infty} h_n e^{2\pi n(z-x_2)/g}) \quad (2)$$

The h_n in this formula are real and h_0 represents the central field value.

It is clear from Eqn. (2) that deviations from a uniform field due to the truncation of the poles or by the manner in which the magnet is excited decay very rapidly if the pole edges are shaped in such a way that $h_{-1} = h_1 = 0$. That is, of course, what one does when one shims a pole. A very sophisticated pole contour would also make h_{-2} and h_2 zero, or very small compared to h_0 , but trying to cancel higher orders would not be worthwhile. It should also be pointed out that the dependence of H_y on y can be used to measure the low order h_n with relative ease by using appropriately made stacks of measuring coils.

If the excitation of the magnet, or the truncation of the poles, violates mid-plane symmetry, one will also have midplane-antisymmetric fields. For such fields H_y is an odd function of y and H_x an even function of y . A consideration similar to the one made above gives for midplane-antisymmetric fields:

$$H^* = \sum_{n=-\infty}^{\infty} b_n e^{\pi(2n+1)z/g} \quad (3)$$

In this formula, the b_n are real, and one can write H^* of course in the same fashion as Eqn. (2). Comparison of Eqn.'s (2) and (3) shows that the most slowly decaying terms in Eqn. (3) decay only half as fast as the slowest terms in Eqn. (2). It should finally be pointed out that Eqn's (2) and (3) can

be applied to many magnets other than dipoles (e.g., strong focussing dipoles, quadrupoles, etc.) by conformally mapping them into dipoles.

4. Magnet Design Considerations

4.1. Properties of the Ideal Lumped Solenoid

The ideal lumped solenoid is (see Fig. B-1 characterized by $\mu = \infty$; by a steel-vacuum interface along the dashed line on the right side of Fig. 1; and by a cylindrical shell at $r_2 = \infty$ to conduct the flux entering along the dashed line around the solenoid.

For symmetry reasons, the distance between the left boundary of the problem and the center of the adjacent coil is $g/2$, and we assume the same distance between the dashed line and the center of the coil adjacent to it. This means that we are dealing with a periodic system of fundamental period length g , so that we need to treat only one cell, indicated by the dotted lines. Because of symmetry the magnetic field must be perpendicular to these lines. The line going through the center of the coil is also a line of symmetry, with the field perpendicular to it as well. To get a qualitative feeling for the fields in the cell, we use the OAM (see Sect. 3a). In it the dotted lines represent insulators, the space between them has a resistivity proportional to the distance r from the center line. The current injected over the cross-section of the coil flows in an easily imaginable pattern to the axis of the system, $r = 0$. While the current density in the OAM is quite non-uniform in the immediate vicinity of the coil, it will obviously smooth out very quickly as one moves toward the axis. A small fraction of the injected current will flow in the vicinity of the symmetry line radially outward, then turn toward the axial direction and, close to the dotted line, flow radially inward. It is quite apparent from this picture that the fields get weak very fast as one moves radially away from the coils. If one were dealing with two-dimensional fields instead of cylindrical fields, the expansion of 2D fields into exponentials (Sect. 3.3) could be directly applied and would yield the result that the dominant term in the description of the field for $r > r_1$, and of the inhomogeneity for $r < r_1$, is proportional to $e^{-2\pi|r-r_1|/g}$. A more detailed 2D model calculation shows that the constant of proportionality for the dominant term equals the average field value H_0 on axis. The fact that we are dealing with cylindrical geometry will obviously modify the details of the decays, but not their basic character. Using again the OAM to see qualitatively the difference between the decay in cylindrical geometry compared to 2D geometry, the fact that the resistivity in the model is proportional to r leads us to conclude that the field outside the coil decays a little faster than indicated above, whereas the field inhomogeneity inside the coil will decay a little slower.

4.2. The Effects Caused by Lumped Return Yokes

If we bring the return flux shell from infinity to a finite value r_2 , we bring steel into a region where the pre-existing field is of the order $H_0 e^{-2\pi(r_2-r_1)/g}$. The resulting field modifications

in that region will be of the same order, and their effect on the field at location r_1 will be cut down by another factor $e^{-2\pi(r_2-r_1)/g}$. We conclude from this that the effect at $r = r_1$ of moving the steel shell to a finite value r_2 is of order $H_0 e^{-4\pi(r_2-r_1)/g}$, i.e. in most cases negligible, provided $(r_2-r_1)/g > 1/4$.

If we now "lump" the return flux shell in the azimuthal direction into "vanes", the details of the field modification are more complicated. If we assume first that the endplates still extend to $r = \infty$, the periodicity in z is not affected by lumping the steel in the azimuthal direction. We therefore still expect field modifications at $r = r_1$ of the order $H_0 e^{-4\pi(r_2-r_1)/g}$, but there will be some dependence on azimuth. If we then reduce the radius of the endplates to $r = r_2$, there will be some additional field modifications. Although the periodicity in z is destroyed by this process, these additional fields will also be extremely small, since the pre-existing fields at the endplates for $r > r_2$ are very small for a reasonable number (≥ 6) of vanes. While it is not too difficult to pursue this argument in more detail, that treatment would go beyond the scope of this report.

If, for a given distance g between coils, it is necessary to obtain a decay of the fields that is faster than $e^{-2\pi(r-r_1)/g}$ outside the coils, one can accomplish this by putting vanes close to the coil and separating them in the azimuthal direction by a distance D somewhat smaller than $g/2$. Under these circumstances, eqn. 3 of Sect. 3.3 will approximately describe the decay of fields between vanes, giving there a most slowly decaying term proportional to $e^{-\pi\Delta r/D}$, with Δr representing the distance from the inside edge of the vanes. In this case, the proximity of the coils could cause local saturation problems in the vanes that would have to be studied in more detail than can be done here.

4.3. Effects Caused by Removal of Steel from Region 1

When removing the steel from region 1 (see Figure 1), i.e., the space between the dashed line and the actually desired steel contour, the field to the left of the dashed line will obviously be reduced over some distance. While this field reduction can be partially compensated by a coil close to steel surface α , the use of that coil does not accurately simulate the field modification caused by the removal of the steel. Instead, we use the following procedure: We first put a magnetic surface charge onto the steel-vacuum interface indicated by the dashed line to the left of region 1. If that surface charge equals the local surface magnetic field value B everywhere, removal of the steel does not change any magnetic fields. We therefore obtain the magnetic field modification everywhere by removing those magnetic charges or, equivalently, by adding the same charges with opposite polarity all along the dashed line to the left of region 1. To see the resulting fields, we use the DAM (see Sect. 3.2 and Table 1), with the vacuum region represented by a 2D sheet with conductivity propor-

tional to r , the steel modeled with perfectly conducting electrodes, and the added magnetic charges represented by current injection from the third dimension. Visualizing the resulting current density and electric field in the 2D sheet, it becomes evident that along the dashed line, the axial field component will be very close to 1/2 of the pre-existing value, and that there will be an increase of the fields all along the inside boundary of the endplate. It should be noted that the increase of the conductivity with r in the DAM indicates that the field modification far from the axis is smaller for cylindrical geometry than it would be in 2D geometry. If the hole that is opened up is comparable to the coil radius r_1 , the fields outside the coils will clearly increase substantially in the end region.

4.4. Effects Caused by Removal of Steel from Region 2

To obtain a qualitative understanding of the field modifications resulting from removal of steel from region 2, we use the same technique as in section 4.3, and should, in fact, apply it simultaneously in the following way: first place appropriate magnetic charges all along the dashed line, remove the steel, and then place charges with opposite polarity on the dashed line and find the resulting fields with the DAM. Since in region 2 the new steel surface is quite close to the old one, most of the injection current in the DAM will flow to the electrode surface representing the new steel surface. Combining that with the fact that the pre-existing field behaves like $e^{-2\pi\Delta r/g}$, one can conclude that the removal of steel from region 2 has only a small effect on the field distribution.

Breaking the endplate into radial spokes is a more drastic modification. Its effect can be visualized also with the magnetic charge - scalar potential surface representation, and it is qualitatively clear that the effects are small provided one uses a reasonable number of spokes (≥ 6) and does not start the spokes closer to the coil than $g/2$.

4.5. Effect of Saturation of Steel

By providing sufficient amounts of steel, saturation of the vanes and the outer part of the endplate can be reduced to any desired level. In the region where the magnetic flux enters the steel one cannot add steel at will. Consequently saturation will occur there above a certain level of excitation, and we want to discuss only the field modification caused by saturation of this part of the steel structure. To do so, we use the method outlined in section 3.1.

It is clear that the flux entering the center part of the endplate (surface β) will produce field lines in the region bounded by surfaces α, β, γ , that are in the same general direction as surfaces α and γ . From this follows that the tangential field component at surfaces α and γ will be considerably larger than its value at surface β . Representing these tangential field components by current sheets, and looking at the polarities of the current in the solenoids, the fields, and the current sheets, it is clear that the current sheet at surface α has the

same polarity as the solenoidal currents, and the current in the sheets at surfaces β and γ has the opposite polarity. We apply now the OAM to see the resulting fields and find the following: Saturation effects on surface α will increase the field in region 1 and its vicinity, while saturation effects on surfaces β and γ will reduce the field over a region that starts near the left edge of region 1 and has an axial size of the order of the outer radius of surface β .

The fields produced by saturation on surfaces β and γ will also have a considerable range in the radial direction. However, the increase of resistivity with r in the OAM indicates that the radial range of these fields is smaller than it would be in 2D geometry.

To keep the proper perspective, one has to remember that the saturation-produced fields are excited by exceedingly weak current sheets unless one drives the steel extremely hard.

REFERENCE

B-1. A. Asner, P. Bossard, Ch. Iselin, Proc. International Symposium on Magnet Technology, Stanford, 1965.

Table B-1. Equivalences Between Quantities In Cylindrical Magnet and Two Analog Models

		1	2	3	4	5	6	7
1	OAM	ρ	$-j_3$	V	-	-	$\vec{e}_3 \times \vec{j}$	$\vec{e}_3 \times \vec{E}$
2	Cyl. Magn	$r\mu$	j_ϕ	rA	rq	V	\vec{H}	$r\vec{B}$
3	DAM	σ	-	-	$-j_3$	V	\vec{E}	\vec{j}

DEFINITIONS:

- ρ = resistivity in the 2D sheet
- σ = conductivity in the 2D sheet
- j_3 = current density injected into the top of the 2D sheet
- \vec{e}_3 = unit vector perpendicular to 2D sheet plane
- V = scalar potential in 2D sheet
- \vec{j}, \vec{E} = current density and electric field in 2D sheet
- j_ϕ = excitation current density in magnet
- q = magnetic charge density in magnet
- μ = permeability of steel
- A = vector potential in magnet
- \vec{H}, \vec{B} = magnetic fields
- r = distance from axis

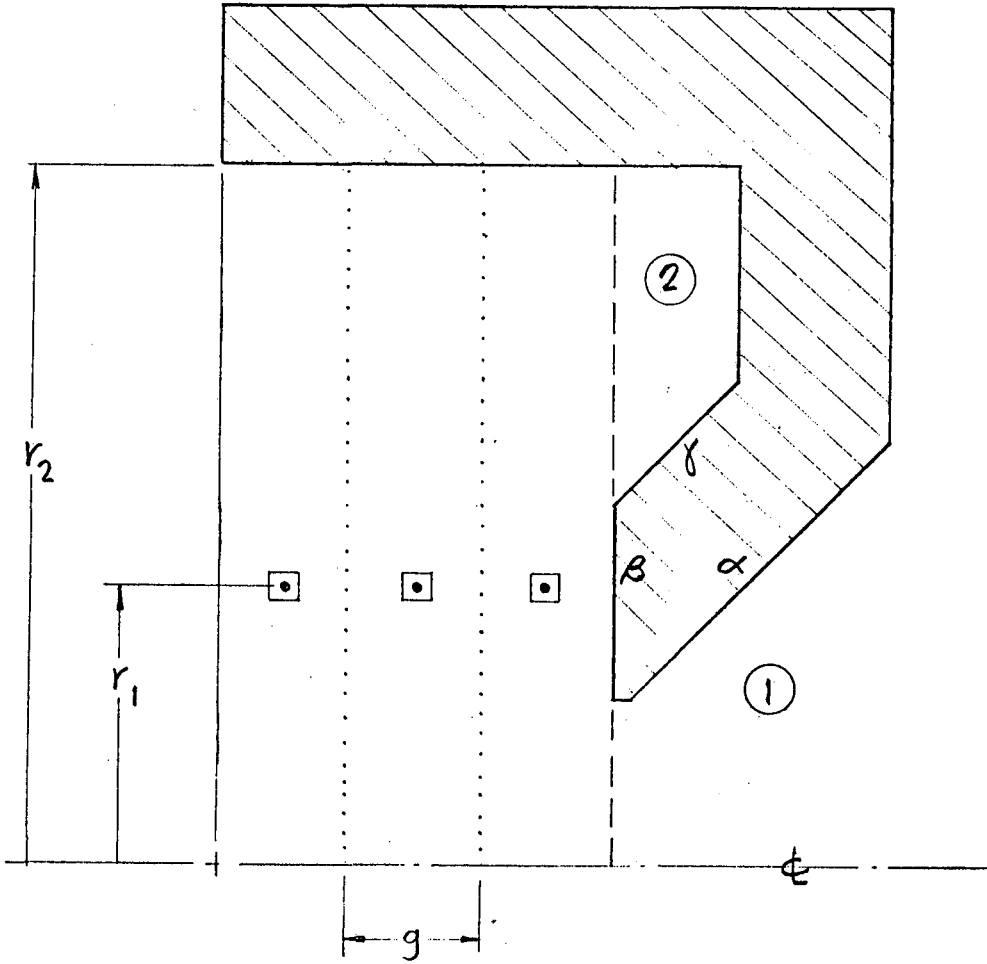


Fig. B-1. Lumped Solenoid Magnet

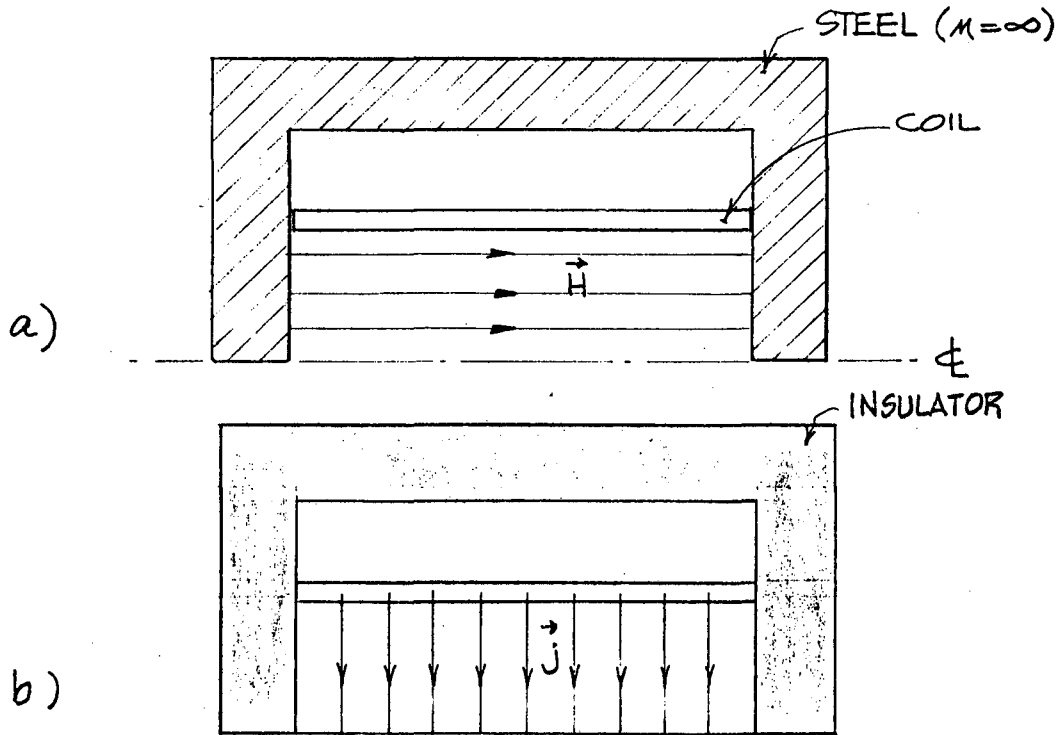


Fig. B-2. Continuous Solenoid in Steel Can

a) \vec{H} -Field in Magnet

b) \vec{j} -Field in OAM

0 0 0 0 2 0 4 4 0 0 0 0

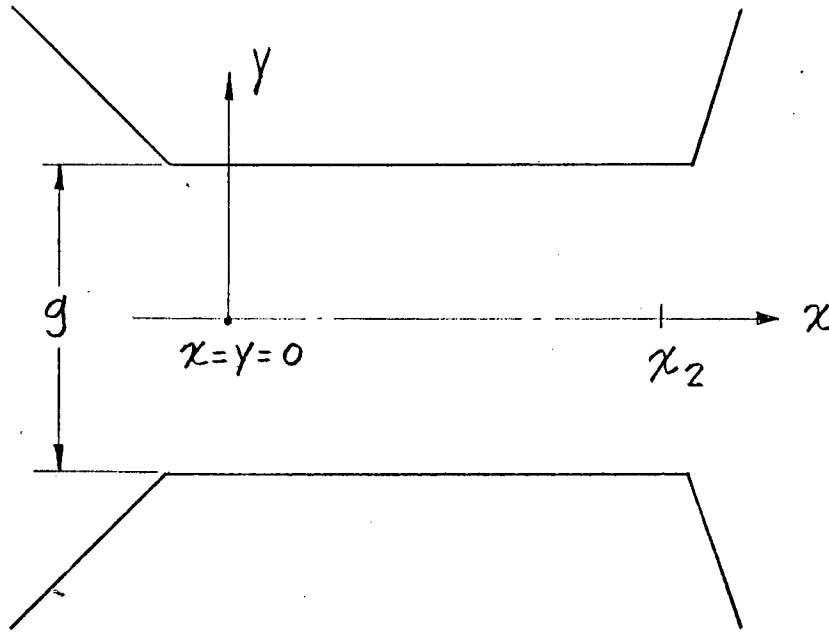


Fig. B-3. Dipole Cross Section

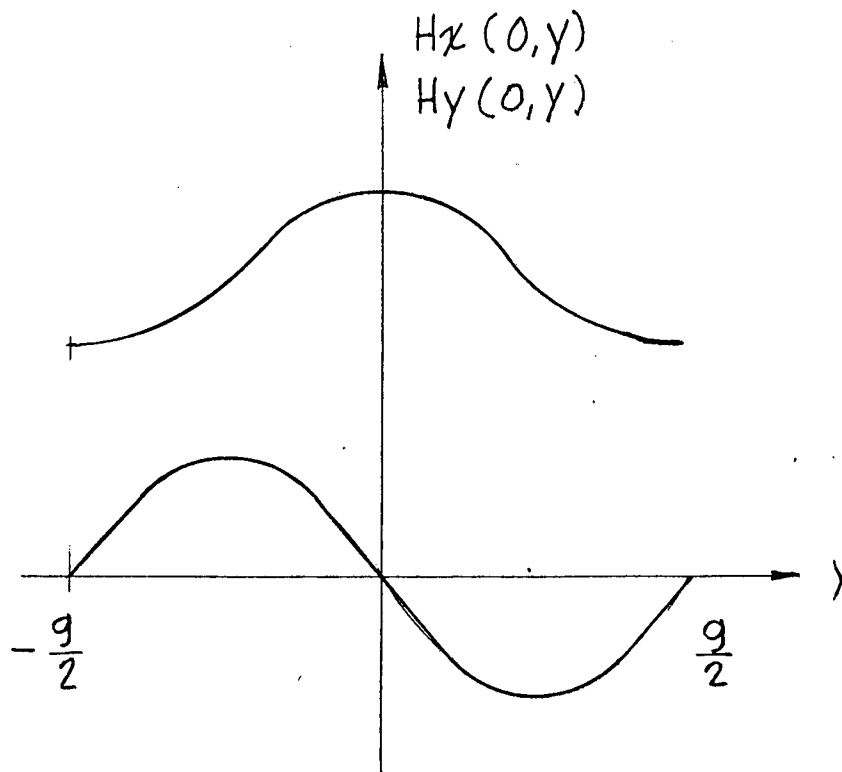


Fig. B-4. Dipole Field Components H_x, H_y vs. y .

—LEGAL NOTICE—

This report was prepared as an account of work sponsored by the United States Government. Neither the United States nor the United States Energy Research and Development Administration, nor any of their employees, nor any of their contractors, subcontractors, or their employees, makes any warranty, express or implied, or assumes any legal liability or responsibility for the accuracy, completeness or usefulness of any information, apparatus, product or process disclosed, or represents that its use would not infringe privately owned rights.

TECHNICAL INFORMATION DIVISION
LAWRENCE BERKELEY LABORATORY
UNIVERSITY OF CALIFORNIA
BERKELEY, CALIFORNIA 94720